IEEE Transactions on Automation Science and Engineering (T-ASE) paper, presented at ICRA 2026, Vienna, Austria.
Cite as T-ASE paper.

Muscle Fatigue-Aware Controller for a Semi-Rigid Knee Exoskeleton

Yifang Zhang, *Member, IEEE*, Jingcheng Jiang, Arash Ajoudani, *Member, IEEE*, and Nikos G. Tsagarakis

***Abstract*—Wearable assistive devices that monitor muscle fatigue reduce the risk of work-related musculoskeletal disorders, enhance rehabilitation outcomes, and extend operational time by optimizing the power consumption of the device. This work proposes a muscle fatigue-aware controller (MFAC) for a semi-rigid knee exoskeleton. During an offline calibration phase, we use Gaussian Process Regression (GPR) to model the relationship between muscle activation (measured via EMG) and the corresponding joint moment and angle, enabling fatigue state estimation for the controller. The trained model then approximates muscle activation online using only joint states and moment derived from user's kinematic data and ground reaction forces provided by the wearable device. The estimated muscle activation is used to assess the muscle fatigue state through a model-based fatigue evaluation module. Notably, EMG measurement is only required during the offline training in our approach, enabling EMG-free online estimation, which significantly enhances the feasibility for long-term mobile applications. Building on muscle fatigue and human–exoskeleton interaction models, we then developed an adaptive controller within a predictive control framework. The resulting optimization problem generates control signals that adjust assistance to reduce the fatigue progression. Two experiments validate the EMG-free fatigue estimation method and the integrated MFAC, demonstrating accurate muscle activation estimation and effective adaptive assistance based on the estimated fatigue state. Analysis of actuator power output reveals adaptivity in which the controller conserves energy during low muscle fatigue and progressively improves power output with increasing fatigue, suggesting a longer duration of the device with a fixed battery capacity.**

***Note to Practitioners*—In industrial environments, many tasks still depend on repetitive human labor, often performed with limited rest and high physical demand. These conditions make workers vulnerable to muscle fatigue, a leading contributor to work-related musculoskeletal disorders. While wearable assistive devices are effective in mitigating fatigue, traditional solutions commonly rely on skin-contact electromyography sensors and deliver fixed assistance levels. Our proposed method avoids the need for such sensors during the operation period and enables adaptive assistance tailored to the user's real-time fatigue condition, thereby ensuring smoother, safer, and more sustainable support for industrial workers. This paper introduces a muscle fatigue-aware controller for a knee exoskeleton that enables adaptive assistance based on the user's fatigue state. One of the contributions is an offline training procedure that uses Gaussian Process Regression to capture the relationship between joint data and muscle activation, avoiding the need for complex biomechanical modeling. Once trained, the system can estimate muscle activation online using only the exoskeleton's built-in motion and force sensors, eliminating the need for fragile and inconvenient electromyography electrodes during daily use. The estimated activation feeds into a model-based fatigue evaluation module, which enables continuous, online EMG-free fatigue monitoring and adaptive adjustment of assistance.Experiments demonstrate that this approach accurately estimates muscle activation, assesses fatigue reliably, and adjusts power output smoothly to balance assistance and device energy efficiency. While current results are limited to controlled laboratory testing with a single joint exoskeleton, the method has potential for broader, long-term use in industrial settings. Potential applications include industrial ergonomics, rehabilitation and sports training.**

***Index Terms*—Fatigue-aware adaptive control, exoskeleton, exosuit, wearable assistive device, muscle activation estimation, muscle fatigue estimation.**

I. Introduction

DESPITE advances in manufacturing technologies over the recent decades, many complex and dynamically changing tasks on production lines still heavily rely on manual human labor [1], [2]. Generally, these tasks involve repetitive motion patterns, insufficient rest time, and forceful manual activities [3]. The prolonged execution of such tasks increases the risk of work-related musculoskeletal disorders (MSDs) [4], which negatively impact individuals, their work performance, and society, while imposing significant costs on employers and public healthcare systems. Among the contributing factors, muscle fatigue is a primary risk for both acute injuries and cumulative disorders [5], [6], [7]. In fact, repetitive tasks, even with a light load, can induce accumulation of local muscle fatigue [8], [9], which can result in injuries and long-term MSDs. Thus, the industry has witnessed increasing demands for new solutions targeting muscle fatigue evaluation and reduction for human operators.

Recently, exoskeletons have been proved effective in reducing muscle fatigue for workers performing industrial tasks. A shoulder exoskeleton significantly reduces fatigue in the

Received 19 May 2025; revised 25 August 2025 and 10 October 2025; accepted 14 November 2025. Date of publication 19 November 2025; date of current version 5 January 2026. This article was recommended for publication by Associate Editor X. Li and Editor Z. Li upon evaluation of the reviewers' comments. This work was supported by European Union's Horizon programmes under Grant 871237 (SOPHIA) and Grant 101070292 (HARIA). *(Corresponding author: Yifang Zhang.)*

This work involved human subjects or animals in its research. Approval of all ethical and experimental procedures and protocols was granted by the Liguria Regional Ethics Committee: Studio IIT-HRII-SOPHIA–N. CER Liguria 554/2020.

Yifang Zhang, Jingcheng Jiang, and Nikos G. Tsagarakis are with the Humanoids and Human Centered Mechatronics (HHCM) Research Line, Istituto Italiano Di Tecnologia (IIT), 16163 Genoa, Italy (e-mail: yifang.zhang@iit.it; jingcheng.jiang@iit.it; nikos.tsagarakis@iit.it).

Arash Ajoudani is with the Human-Robot Interfaces and Interaction (HRI^2) Research Line, Istituto Italiano Di Tecnologia (IIT), 16163 Genoa, Italy (e-mail: arash.ajoudani@iit.it).

Digital Object Identifier 10.1109/TASE.2025.3634838

IEEE Transactions on Automation Science and Engineering (T-ASE) paper, presented at ICRA 2026, Vienna, Austria.

anterior deltoid muscle during overhead activities [10]. Similarly, [11] reported that a soft exoskeleton (exosuit) can mitigate muscle fatigue in the lumbar multifidus, iliocostalis lumborum, and longissimus thoracis muscles of the lower back. Additionally, [12] showed that a knee exoskeleton effectively reduces quadriceps muscle fatigue across a variety of tasks. However, in most studies, muscle fatigue is treated merely as a metric to assess exoskeleton performance, rather than as an input for real-time adaptive control.

To develop a muscle fatigue-aware controller for an assistive exoskeleton, the first step is to select a method for identifying the muscle fatigue state. Over the past decades, various models have been explored to evaluate muscle fatigue. The most precise approaches involve modeling physiological mechanisms including Ca^{2+} cross-bridge cycling [13], motor unit activation [14], and the relationship between muscle force and intracellular pH [15], all of which are closely tied to muscle function. However, physiological models require complex and specialized modeling procedures which are impractical for occupational ergonomics applications. Alternatively, muscle fatigue can be estimated by analyzing the shift in median frequency of the electromyography (EMG) signal. Research shows that as muscle fatigue increases, the median frequency of the EMG signal decreases, while its amplitude rises [16]. Although EMG method works effectively under conditions of constant muscle contraction, it becomes unreliable and inconsistent for tasks involving dynamic movements [17].

To extend muscle fatigue evaluation to dynamic tasks in ergonomics, Ma et al. [18] proposed a simple dynamic fatigue model that also incorporates a recovery component, drawing on earlier formulations [19], [20]. The model uses the current exertable maximum force capacity of the muscle as an indication of muscle fatigue, showing promising results for assessing muscle fatigue under both static and dynamic conditions. However, it requires muscle force or joint torque as input, which cannot be measured directly. Applying the model in real-world scenarios, therefore, necessitates complex calibration and biomechanical modeling, typically involving human kinematic chain modeling and the use of external force sensors to estimate joint torques. Muscle activation can then be estimated by dividing the computed joint torque by the corresponding joint moment arm [15]. This approach, however, introduces significant challenges. Human joints vary across individuals due to their nonuniform articular surfaces [21], joint moment arms are not constant during motion, and inter-individual differences can be considerable [22]. For example, accurately modeling the biomechanics of the knee joint requires MRI imaging [23], which is both time-consuming and costly.

In addition to computational approaches for estimating muscle state in fatigue assessment, direct measurement methods have also been explored. Inspired by the RC circuit dynamic, Peternel et al. [17] proposed a low-complexity EMG-based muscle fatigue model that directly uses the normalized EMG signal as an indicator of muscle activation. His model demonstrates a similar exponential response as Ma's model [24]. The model takes the normalized muscle effort level measured from the EMG signal and directly outputs a fatigue index, which changes between $[0, 1]$, indicating full rest or fatigue state. This model has been further applied for muscle fatigue estimation and for controlling assistance in human–robot collaboration tasks. Beyond EMG, ultrasound has also been employed for continuous estimation of muscle fatigue state [25], by capturing fatigue-induced nonlinear muscle thickening patterns. However, EMG sensing presents certain drawbacks, as its accuracy is highly sensitive to factors such as electrode placement, body movement, skin sweat, and body hair [26]. Similarly, ultrasound is sensitive to motion artifacts and probe placement, and it requires bulky, complex equipment, making it suitable primarily for stationary applications and impractical for mobile or wearable use.

To enable the practical and long-term use of wearable assistive devices with the proposed fatigue-aware controller in industrial settings, we extend the muscle fatigue estimation approach from previous work [17]. Specifically, the input of online EMG-based muscle activation is replaced with an estimated value obtained from an offline-trained GPR model. In this way, EMG signals are required only during the user's initial calibration phase for offline training, eliminating the need for delicate and inconvenient EMG measurements throughout the entire usage process for online estimation. As a result, the sensing complexity of the assistive device remains unchanged, while still enabling reliable online muscle activation prediction and continuous fatigue estimation.

Several studies have reported the integration of fatigue models into the control algorithms of various assistive devices. For instance, in the field of human–robot co-manipulation, fatigue has typically been used as a binary trigger to activate assistance once a predefined threshold is reached [17], [27]. In the domain of exoskeletons, Del-Ama et al. [28] proposed a cooperative control strategy for a hybrid exoskeleton combining robotic actuation with functional electrical stimulation (FES), where muscle fatigue was estimated using the torque–time integral (TTI) to adapt assistance and balance power contributions between the user's muscles and the exoskeleton during walking rehabilitation. Sheng et al. [29] developed a hybrid knee exoskeleton that leverages real-time ultrasound imaging to estimate muscle fatigue and dynamically regulate assistance. More recently, Bergmann et al. [30] introduced a three-compartment controller fatigue model and integrated it into a human-in-the-loop (HiL) control system that adjusts assistance based on both subjective fatigue ratings and objective MVC decline.

The control strategies presented in [17], [27], and [29] rely on a binary switching mechanism, where robotic assistance is either fully engaged or disengaged once a predefined fatigue threshold is reached. This approach is effective in co-manipulation scenarios, where external loads can be entirely handled by the robotic manipulator, or in FES-based rehabilitation, where muscle activation is directly controlled. In such contexts, switching assistance on or off does not cause significant discomfort arising from asynchrony between voluntary motor intention and robotic support. However, this binary paradigm is not suitable for long-term use in augmentative exoskeletons designed for performance enhancement. In contrast, the strategies proposed in [28] and [30] modulate

IEEE Transactions on Automation Science and Engineering (T-ASE) paper, presented at ICRA 2026, Vienna, Austria.

assistance continuously as a function of fatigue. Yet, the controller in [30] is tailored to rehabilitation training, where resistance is intentionally applied at low fatigue levels to accelerate fatigue development, while the method in [28] was designed to balance FES intensity and robotic support during rehabilitation walking. Consequently, neither approach can be directly transferred to assistive exoskeletons intended for sustained industrial use, as they were designed for short-term, supervised rehabilitation or co-manipulation tasks, where binary or fatigue-inducing assistance is acceptable. Industrial exoskeletons use, in contrast, require continuous, adaptive, and ergonomically synchronized assistance to ensure comfort, stability, and sustained performance over prolonged time. Controllers optimized for short, repeatable rehabilitation exercises often fail to generalize to these complex, variable, and long-term conditions that may appear in the industrial use-case.

To this end, this work integrates the muscle fatigue estimation model into a constrained optimization–based adaptive controller, which provides safe, tunable, and continuous assistance according to the user's fatigue state. Experimental results demonstrate that the proposed muscle activation estimation method achieves sufficiently accurate predictions, while the integrated fatigue model enables continuous and reliable monitoring in both static and periodic motions, with performance comparable to EMG-based estimation. The controller ensures smooth, adaptive assistance across these activities.

Furthermore, the MFAC allows the assistive device to adapt its support according to the user's fatigue level: reducing assistance to conserve energy when fatigue is low, when the risk of work-related musculoskeletal disorders is minimal, and increasing assistance when fatigue is high, thereby providing greater support despite higher energy expenditure. By incorporating the user's fatigue state into the control strategy, the MFAC enhances energy efficiency and has the potential to extend the device's operating time on a single battery charge.

The rest of the paper is organized as follows. Section II describes the methodologies in our work. Section III introduces two experiments for training and validating the GPR-based muscle activation estimation model and the evaluation of the proposed muscle fatigue-aware controller when it works with the Exo-Muscle device. Finally, Section IV draws the conclusion and briefly discusses future work activities.

II. Methodology

This section introduces the details of the proposed EMG-free muscle activation estimation, muscle fatigue evaluation method, and muscle fatigue-aware adaptive controller (MFAC). An overview schematic of the online EMG-free muscle fatigue evaluation method is introduced in Fig. 4. The method is applied to assess the level of muscle fatigue in the quadriceps when utilizing a knee assistive device known as Exo-Muscle, shown in Fig. 1 and on the left side of Fig. 4. Section II-A briefly describes this human-assistive device and outlines its modeling, which enables the extraction of knee joint state and torque information from the inherent sensing system of the assistive device. Subsequently, Section II-B introduces the muscle fatigue estimation model [17] utilized

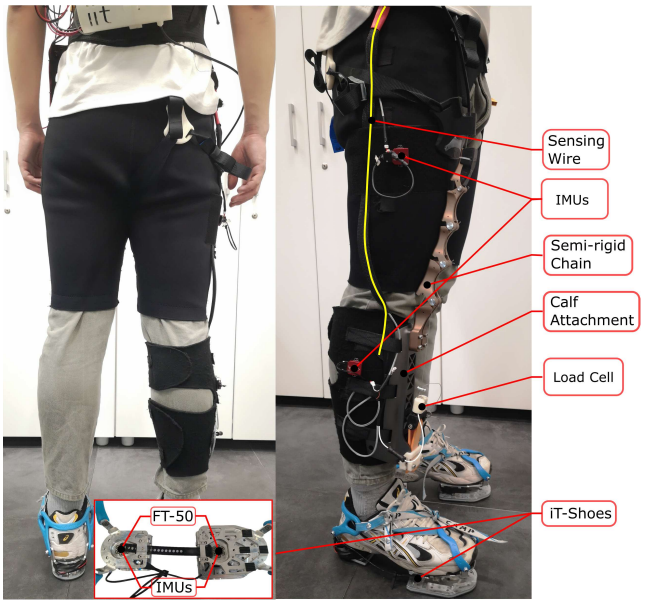

Fig. 1. Main features of the Exo-Muscle knee assistive device.

in this study and schematically shown on the right side of Fig. 4. To overcome the need for electromyography (EMG) measurements employed in [17] to obtain muscle activation as input to the fatigue model, this work instead proposes to use as input for the muscle fatigue model the output of a trained muscle activation estimation model (yellow block in the middle of Fig. 4) that incorporates the learned latent relationship between joint state information from Section II-A and muscle activation measured by EMG. The learning method (GPR) used in this study and the training procedures are elaborated in Section II-C. The last Section II-D elaborates on MFAC, an optimization-driven adaptive controller developed on the basis of the modeling of the human-exo system and the muscle fatigue model.

A. Human-Exo Modelling

The assistive device used in this work is the Exo-Muscle knee assistive system, which aims to provide torque compensation for knee extension. Thus, the scope of this work focuses on the implementation and validation of the proposed EMG-free muscle activation estimation method and adaptive controller on the lower limb and, in particular, on the knee joint and the related quadriceps muscles.

To evaluate the user's state, control the assistive device, and train the muscle activation estimation model, the human–robot system must be modeled. As in our previous work, we estimate knee joint torque using the ground reaction forces and the lower-limb kinematics [31]. However, different from the previous work, the ground reaction force in this study is measured by the iT-Shoes [32](as shown in Fig. 1). The use of iT-Shoes ensures that the subject can perform more complex tasks, such as stair stepping.

The lower limb system is modelled with a Unified Robot Description Format (URDF) model, which can be scaled for different persons. As joint moment are computed with

IEEE Transactions on Automation Science and Engineering (T-ASE) paper, presented at ICRA 2026, Vienna, Austria.

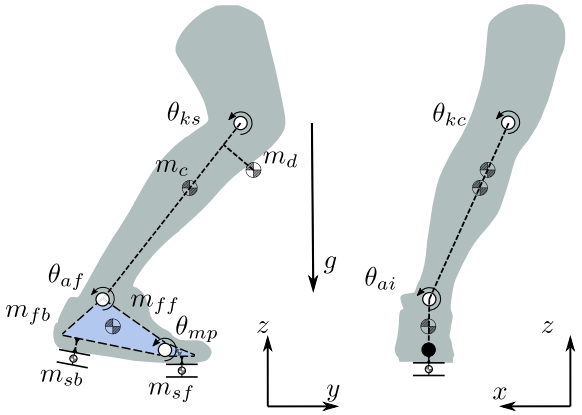

Fig. 2. Modeling of lower limb.

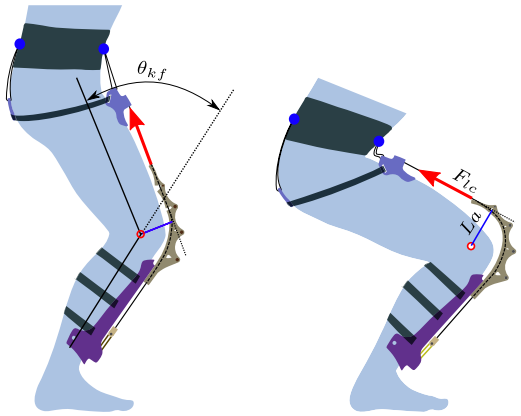

Fig. 3. Simplified assistance principle of the Exo-Muscle.

ground reaction forces, the URDF only need contains the body segments and assistive device elements, which are below the human knee joint. These include the feet, calf, iT-Shoes, and some components of the Exo-Muscle device. As shown in Fig. 2, the system is modeled with 3 human links (calf, back foot and front foot) of a mass of m_c, m_{fb}, m_{ff} respectively. The mass m_{sb} of the back side of the shoes and the mass m_{sf} of the front side are attached at the bottom of the back and front part of the foot. As shown in Fig. 3, the Exo-Muscle is attached to the front of the calf, and its mass is denoted as m_d in Fig. 2. In the standard URDF model, the lengths of human segments and the locations of the centres of mass are defined based on [33] and [34]. When deployed for computation and control, the model is scaled using the measured height and weight of the users.

The metatarsophalangeal (MTP) joint is modeled with one degree of freedom (DoF), denoted as θ_{mp}. The ankle joint is modeled with two DoFs corresponding to dorsiflexion–plantarflexion and inversion–eversion, denoted as θ_{af} and θ_{ai}, respectively. Similarly, the knee joint is modeled with two DoFs representing motion in the sagittal and coronal planes, denoted as θ_{ks} and θ_{kc}, respectively. Joint states are measured using the Euler angle interface provided by IMUs (VN-100, VectorNav) attached to the thigh, calf, and the front and rear parts of the iT-Shoe.

At system startup, the IMU readings are initialized while the user is standing upright. During operation, the metatarsophalangeal joint angle θ_{mp} is extracted from the IMUs mounted on the front and rear parts of the iT-Shoes. The ankle joint angles, θ_{af} and θ_{ai}, are obtained from the IMUs located on the calf and the rear part of the iT-Shoes. Specifically, the knee joint angles θ_{ks} and θ_{kc} are directly measured using the IMU attached to the calf. The joint states are represented with a vector

$$\mathbf{q} = [\theta_{mp}, \theta_{af}, \theta_{ai}, \theta_{ks}, \theta_{kc}]^T \tag{1}$$

The ground reaction forces for each foot are measured using two 6-axis force/torque (FT) sensors embedded in the iT-Shoe—one positioned at the front and the other at the rear, as shown in Fig. 1. Each sensor is based on semiconductor strain gauges, providing low noise and high structural stiffness. They measure forces (f_x, f_y, f_z) within a range of $\pm$2000 N and torques (τ_x, τ_y, τ_z) within a range of $\pm$40 Nm, with a resolution of 500 mN for forces and 20 mNm for torques [32]. The forces and torques measured by these two sensors are denoted as

$$\begin{aligned} \mathbf{f_{grf}} &= [f_{fx}, f_{fy}, f_{fz}, \tau_{fx}, \tau_{fy}, \tau_{fz}]^T \\ \mathbf{f_{grb}} &= [f_{bx}, f_{by}, f_{bz}, \tau_{bx}, \tau_{by}, \tau_{bz}]^T \end{aligned} \tag{2}$$

where sub-index gr denotes the ground reaction. The f and b indicate the data from the front and back parts of the shoes. The force pair $\mathbf{f_{grb}}$ and $\mathbf{f_{grf}}$ are considered as external loads and applied at the center of each force-torque sensor. In real operation scenarios, the calf is rarely in contact with external objects. Thus, except for the ground reaction force, we assume there is no extra reaction force applied to the system. In addition, as the mass and inertia of these parts is relatively low compared with that of the whole system, and the value of velocity and acceleration of these parts are small when the foot is in contact with the ground, the dynamics terms of these parts are ignored. As a result, this leads to the dynamic model

$$\boldsymbol{\tau} = -(\mathbf{G(q)} + \mathbf{J(q)}_\mathbf{f}^\mathbf{T} \cdot \mathbf{f_{grf}} + \mathbf{J(q)}_\mathbf{b}^\mathbf{T} \cdot \mathbf{f_{grb}}) \tag{3}$$

where $\boldsymbol{\tau}$ denotes the vector of the joint moment, $\mathbf{G(q)}$ is the Gravity term represented in the joint space and $\mathbf{J(q)_f}$ and $\mathbf{J(q)_b}$ represent the Jacobian for the front and back parts of the force shoes, respectively. By solving (3), τ_{kf} representing the total knee moment is obtained. To be noted that for the training the muscle activation estimation model, the training data is collected without the Exo-Muscle mounted on the leg of the human subjects. Thus, the mass of the Exo-Muscle is not included in the URDF model, while it is added in the second set of experiments, where the device is worn by the human operator.

Therefore, in Section II-C, the muscle activation estimation model is trained using the knee internal torque $\hat{\tau}_{kf}$ without considering the assistive device and any assistance (human subjects are not wearing the device during the collection of the training dataset). As a benefit, the trained model can potentially be used for robot assistance scenarios with different devices, as long as $\hat{\tau}_{kf}$ is given as input to the model. To this end, in the training dataset, $\hat{\tau}_{kf}$ is equal to τ_{kf}, as the Exo-Muscle is not mounted during the training phase. However, when operated with the robot, the contribution of the assistance

IEEE Transactions on Automation Science and Engineering (T-ASE) paper, presented at ICRA 2026, Vienna, Austria.

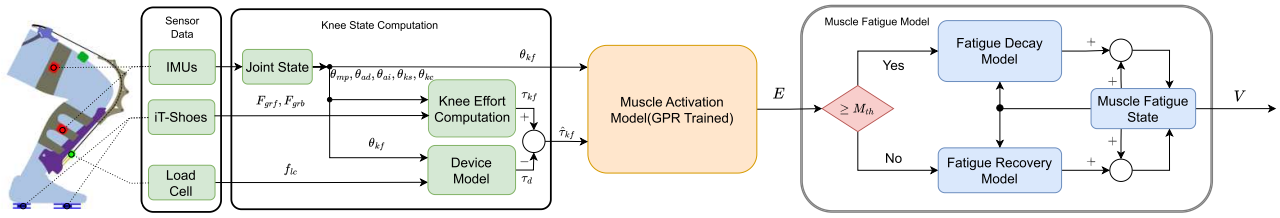

Fig. 4. The schematic illustrating the proposed online muscle activation estimation and fatigue evaluation approach, which operates without EMG, and their interaction with the Exo-Muscle device's sensing and knee state computation block.

device, τ_d, needs to be computed to derive $\hat{\tau}_{kf}$. Figure. 3 shows the simplified assistance principle of the tendon-driven Exo-Muscle. The tension force (F_{lc}) on the tendon is measured with a load cell shown in Fig.1 and adjusted by controlling an actuator to pull/release the Bowden tendon. The semi-rigid chain (shown in both Figure. 1 and Fig. 3) creates a predefined guiding route for the Bowden tendon and forms a moment arm (L_a) relative to the knee joint rotation center. Consequently, the Exo-Muscle generates an assistive torque τ_d for the knee joint. Therefore, in the Exo-Muscle assistance mode, the knee internal torque $\hat{\tau}_{kf}$ is written as

$$\hat{\tau}_{kf} = \tau_{kf} - \tau_d \tag{4}$$

where τ_{kf} is solved by Equation (3). In this work, L_a is represented by a fitted polynomial equation, where the variable θ_{kf} denotes the knee flexion angle. Specifically, $L_a(\theta_{kf})$ describes the moment arm of the tension force relative to the knee's center of rotation as a function of knee flexion. The detailed derivation procedure is provided in [31]. The resulting expression for $L_a(\theta_{kf})$ is given by:

$$\begin{aligned} L_a(\theta_{kf}) = &-2.271 \cdot 10^{-12}\,\theta_{kf}^5 + 1.096 \cdot 10^{-9}\,\theta_{kf}^4 \\ &- 2.462 \cdot 10^{-7}\,\theta_{kf}^3 + 2.870 \cdot 10^{-5}\,\theta_{kf}^2 \\ &- 1.012 \cdot 10^{-3}\,\theta_{kf} + 0.074 \end{aligned} \tag{5}$$

In this study, the knee flexion angle θ_{kf} is obtained using IMU sensors mounted on the thigh and calf segments. Then τ_d is formulated as

$$\tau_d = F_{lc} \cdot L_a\left(\theta_{kf}\right) \tag{6}$$

However, here, we only present the essential actuation principles and computations when using the Exo-Muscle device. For more details on the design, modeling and control of the Exo-Muscle, please refer to [31].

B. Muscle Fatigue Model

To estimate human muscle fatigue, various models have been proposed in previous studies [14], [15], [35]. Most of these models depend on precise modeling of the human actuation mechanism and require complex calibration before use. To improve applicability in real-world scenarios and enable continuous fatigue estimation, Ma et al. [24] proposed a simplified model. However, their approach still relies on muscle load estimation obtained through inverse dynamics and a complex biomechanical model.

Considering that the relationship between human effort and EMG signals can be approximated as linear within a certain

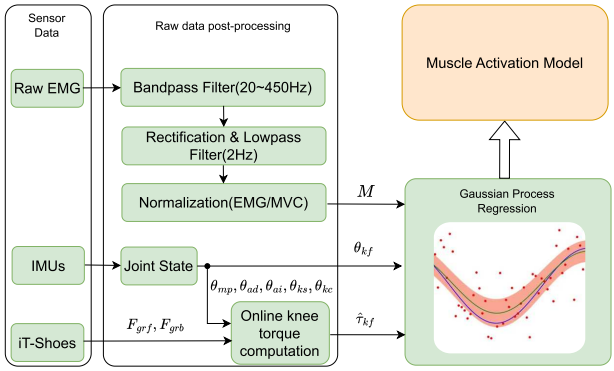

Fig. 5. Training process of the proposed muscle activation estimation model.

operating range [36], [37], Peternel et al. [17] extended Ma's model [24] by proposing a low-complexity EMG-based muscle fatigue model. In this approach, the muscle force input of fatigue estimation model is replaced with a measured muscle activation index M, representing the normalized EMG signal. It is written as

$$0 \le M = \frac{EMG}{MVC} \le 1 \tag{7}$$

where the *EMG* denotes the post-processed EMG signal (as shown in Fig. 5), while the *MVC* represents the *EMG* reading at maximum voluntary contraction.

This method significantly reduces the complexity of muscle fatigue estimation, as it directly measures muscle activity and eliminates the need for extensive sensing and modeling of the human biomechanical system. It is composed of two fundamental components: the fatigue decay model and the fatigue recovery model, expressed as

$$\frac{dV(t)}{dt} = \begin{cases} (1 - V(t))\dfrac{M}{C_F}, & M \ge M_{th} \\ -V(t)\dfrac{R}{C_F}, & M < M_{th} \end{cases} \tag{8}$$

where $V(t)$ denotes the muscle fatigue index, ranging from 0 to 1, with higher values indicating greater fatigue. Parameters C_F and R characterize muscle-specific properties related to fatigue and recovery, and should be tuned according to the individual subject and the target muscle involved in the given task. The M denotes the continuously measured muscle activation level, obtained using (7).

The fatigue model is integrated into an online estimation framework and visualized within the Muscle Fatigue Model

IEEE Transactions on Automation Science and Engineering (T-ASE) paper, presented at ICRA 2026, Vienna, Austria.

block in Fig.4. It should be noted that, in the schematic, the input of the fatigue model is denoted as E, which corresponds to the estimated muscle activation level derived from the trained model in Fig.5.

With the fatigue decay model of (8), the following exponential response can be derived

$$V(t) = 1 - \exp^{-\int \frac{M}{C_F} dt} \tag{9}$$

Considering the time constant properties of (9), the constant C_F can be obtained by a set of preliminary endurance experiments. In the experiments, human subjects are instructed to perform activities requiring different muscle activation levels M_{ref} (In this study, three muscle activation levels are considered: 0.2, 0.5 and 0.7) until they can not endure anymore. The endurance time T_{end} for each test is recorded. At T_{end}, we assume a fully developed muscle fatigue state with the muscle fatigue index $V = 0.993$, representing the system's response at five times the time constant. We can then fit the data to the (10), which is extracted from (9).

$$C_F = -\frac{M_{ref} \cdot T_{end}}{\log(1 - 0.993)} \tag{10}$$

Eventually, a value of C_F is obtained for each M_{ref}, and the average of these values is used as a constant in (8). For the recovery rate R, a conservative value of $R = 0.5$ is reported in [17]. Alternative selections of R can be found in [18].

In contrast to the implementation in [17], which directly uses real-time EMG measurements as input to the muscle fatigue model, this study replaces the muscle activation M with the approximated value E obtained from the GPR-trained model (Fig. 4). As a result, the estimation approach eliminates the need for complex pre-calibration procedures associated with biomechanical system modeling and removes the requirement for EMG signals in online fatigue estimation. The details of the GPR-trained approximation model are presented in Section II-C.

C. GPR Based Muscle Activation Approximation

As discussed in the previous section, the muscle fatigue estimation model uses the muscle activation index M as input, whereas in [17], the input is the normalized EMG signal. However, the EMG signal measurement is sensitive and can be influenced by the conditions of the environment and human factors, making the direct use of the EMG signal as the input of the model in real scenarios impractical, inconvenient, or uncomfortable for the workers. On the other side, the muscle force can also be derived by considering the transmission mechanism model of the joint. However, this is a complex and difficult approach. To precisely model the relation of internal moment arm and knee angle for each user, a non-invasive technology such as magnetic resonance imaging should be used, which is expensive in time and cost. To enable practical, industrial use of muscle fatigue estimation, we propose a solution based on GPR to model the relationship between knee joint state (torque and angle) and corresponding muscle activation M. As a result, we can eliminate the EMG sensor and replace M with an estimated muscle activation index, E. This estimation relies solely on joint state and torque data, which are measured and computed using the sensors (IMUs and iT-Shoes) integrated into the Exo-Muscle assistive device.

The workflow for training the muscle activation estimation model with GPR method is presented in Fig. 5. In the first step, we need to prepare the training dataset for the GPR. To compensate for the knee torque induced by gravity, the muscles Vastus Intermedius, Vastus Lateralis, Vastus Medialis, and Rectus Femoris contract together to create the internal torque. When generating a certain knee extension torque, these muscles exhibit a minor difference in their activation index, yet they demonstrate a similar changing trend during contraction [37], [38]. This provides an opportunity to simplify the problem by utilizing the EMG signal from one of these muscles to indicate the activation of the muscle group, offering the benefit of easier implementation in real-world application scenarios. Eventually, in this study, the EMG signal from Vastus Lateralis is selected and measured using the Delsys Bagnoli system. Subsequently, as shown in Fig. 5, the EMG signal is band-pass filtered, rectified, and low-pass filtered to reduce noise and extract the envelope. The normalized muscle activation M is then computed using (7). In the meantime, the corresponding $\hat{\tau}_{kf}$ and θ_{kf} are computed and recorded.

The data set with n data points is prepared and denoted as

$$\mathbf{D} = \left\{x_i, y_i\right\}_{i=1}^{n} \tag{11}$$

where $\mathbf{x}_i$ denotes the input vector of i^{th} data pair, while the y_i indicates the corresponding muscle activation index. Each input vector includes two variables

$$\mathbf{x}_i = \left\{\hat{\tau}_{kfi}, \theta_{ki}\right\} \tag{12}$$

where the $\hat{\tau}_{kfi}$ and θ_{ki}, denote the knee internal torque and knee flexion angle, respectively. The dataset $\mathbf{D}$ will be used to learn the latent function, which transforms the input vector $\mathbf{x}_i$ to the target value y_i. The unknown transformation can be written as

$$y_i = f(\mathbf{x}_i) + \epsilon_i \tag{13}$$

where the $f(\mathbf{x})$ represents a Gaussian distribution

$$f(\mathbf{x}) \sim N(m(\mathbf{x}), k(\mathbf{x}, \mathbf{x}')) \tag{14}$$

with its mean function $m(\mathbf{x})$ and covariance function $k(\mathbf{x}, \mathbf{x}')$. The ϵ_i indicates the Gaussian noise, which has zero mean and variance σ_n^2. As a result, the learned function modelled with a multivariable Gaussian is formulated as

$$P(\mathbf{f}|\mathbf{X}) \sim N(\mathbf{f}|\mathbf{m}, \mathbf{K} + \sigma_n^2 I) \tag{15}$$

In this study, the RBF kernel, which is the most widely used kernel, is taken. The general RBF kernel function is given as

$$k(\mathbf{x_i}, \mathbf{x_j}) = \sigma_f^2 exp\left(-\frac{1}{2l}(\mathbf{x_i} - \mathbf{x_j})^T(\mathbf{x_i} - \mathbf{x_j})\right) \tag{16}$$

where σ_f denotes the signal variance and l represents the length scale of the kernel. Their values are obtained by maximizing the log marginal likelihood. To predicate y_* with the new input query point x_*, the joint distribution of the trained dataset and query point is given as

$$\begin{pmatrix} \mathbf{y} \\ y_* \end{pmatrix} \sim N\left(\mathbf{0}, \begin{bmatrix} \mathbf{K}(\mathbf{X}, \mathbf{X}) + \sigma_n^2 \mathbf{I} & \mathbf{K}(\mathbf{X}, \mathbf{x}_*) \\ \mathbf{K}(\mathbf{x}_*, \mathbf{X}) & K(\mathbf{x}_*, \mathbf{x}_*) \end{bmatrix}\right). \tag{17}$$

IEEE Transactions on Automation Science and Engineering (T-ASE) paper, presented at ICRA 2026, Vienna, Austria.

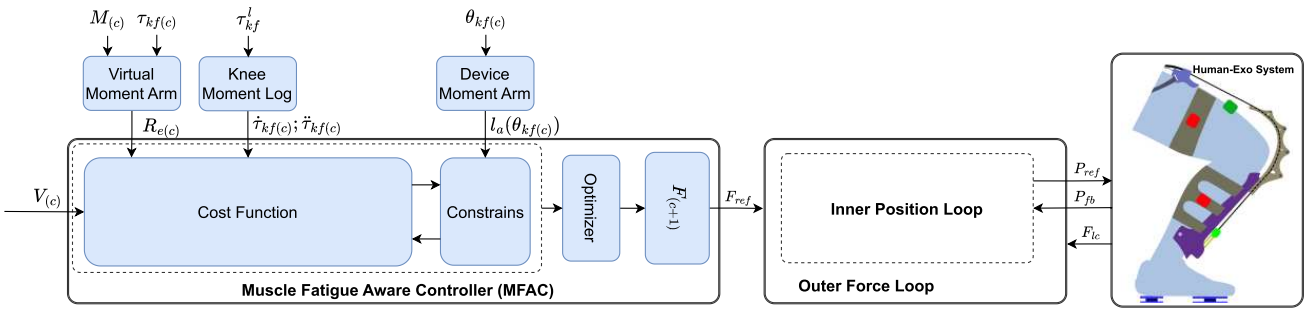

Fig. 6. The control schematic includes MFAC and the lower-level force-position controller.

Then we can yield the predicted mean value μ_*

$$\mu_* = \mathbf{K}(\mathbf{x}_*, \mathbf{X})[\mathbf{K}(\mathbf{X}, \mathbf{X}) + \sigma_n^2 I]^{-1}\mathbf{y} \tag{18}$$

Finally, the trained model is integrated into Fig. 4 for online muscle fatigue evaluation. The estimated muscle activation index E represents the predicted μ_*. The training of the model is performed offline in Python using the machine learning package scikit-learn.

D. Muscle Fatigue Aware Controller

In our previous work [31], the developed semi-rigid exoskeleton is controlled using a low-level force controller with an inner position loop. Concurrently, the force reference is generated based on a predefined percentage of knee moment compensation, computed through inverse dynamics. Leveraging on the models presented in Section II-B and Section II-C, we propose an improved muscle fatigue-aware controller (MFAC) to generate a tension force reference, as illustrated in Fig.6. By replacing the muscle activation input of the muscle fatigue model with the trained muscle activation estimation model from SectionII-C, the MFAC eliminates the need for real-time EMG measurements, thereby improving the feasibility of long-term, mobile operation of the device.

The MFAC is an optimization-based controller developed based on the architecture of Model Predictive Control. In the controller, the muscle fatigue V is the system state we would like to regulate, while the system control input is defined as p, which is the percentage of the knee torque we would like to compensate.

As the muscle fatigue model (8) includes a fatigue decay and a recovery model, the discrete-time state equation can be expressed in two forms—one for the decay state and one for the recovery state. In this notation, the subscript c denotes the current discrete-time step, and i represents the i^{th} step in the prediction horizon.

The fatigue decay stage is

$$V_{(c+i)} = (1 - V_{(c+i-1)})\frac{E_{(c+i)}}{C_F} \cdot \Delta t + V_{(c+i-1)} \tag{19}$$

while the recovery stage is

$$V_{(c+i)} = -V_{(c+i-1)}\frac{R}{C_F} \cdot \Delta t + V_{(c+i-1)} \tag{20}$$

In the real-time control of the assistive device, the optimization is performed at each control loop. To avoid discontinuities, the fatigue state for each step in the prediction horizon must be selected before optimization and remain fixed during the process. Therefore, in this study, a single stage is used to construct the optimization problem for each loop. The selection of the fatigue stage depends on the most recent estimated $E_{(c)}$. If $E_{(c)}$ exceeds the predefined threshold M_{th}, the equation in (19) will be applied, otherwise, the equation in (20) will be used.

In (19), the $E_{(c+i)}$ is the estimated muscle activation level in the predicate horizon. To define the $E_{(c+i)}$ in the predicate horizon, the total knee moment needed for each step in the predicate horizon needs to be approximated for each step. Typically, the device is expected to operate under quasi-static conditions, where knee moment changes smoothly within the predictive horizon. Thus, the knee torque at the i^{th} step of the prediction horizon is expressed using a second-order recursive Taylor expansion:

$$\tau_{kf(c+i)} \approx \tau_{kf(c+i-1)} + \dot{\tau}_{kf(c)} \cdot \Delta t + \frac{1}{2}\ddot{\tau}_{kf(c)} \cdot (\Delta t)^2 \tag{21}$$

The quantities $\dot{\tau}_{kf(c)}$ and $\ddot{\tau}_{kf(c)}$ represent the first-order and second-order derivatives of the knee torque at the initial time. In this work, their values are determined by averaging the changes observed in previously logged data, which records measurements of τ_{kf} for steps of the same length N as the prediction horizon. It should be noted that the use of second-order derivatives in recursive computation may introduce instability into the optimal controller, particularly in the presence of rapid motions or noise from wearable sensors. To enhance robustness for more complex motions and tasks, one could consider applying a clipping function to bound $\dot{\tau}_{kf(c)}$ and $\ddot{\tau}_{kf(c)}$, or alternatively, reducing the recursive computation to a first-order Taylor expansion. However, this study is conducted under quasi-static conditions, which do not involve rapid motion changes; therefore, the second-order Taylor expansion is preserved.

The logged τ_{kf} is denoted as

$$\tau^{l}_{kf} = \begin{bmatrix} \tau_{kf(c-N+1)} \\ \vdots \\ \tau_{kf(c-1)} \\ \tau_{kf(c)} \end{bmatrix}; N \times 1 \tag{22}$$

IEEE Transactions on Automation Science and Engineering (T-ASE) paper, presented at ICRA 2026, Vienna, Austria.

then the $\dot{\tau}_{kf(c)}$ and $\ddot{\tau}_{kf(c)}$ can be denoted as

$$\begin{aligned}\dot{\tau}_{kf(c)} &= \frac{\tau^l_{kf}[N] - \tau^l_{kf}[1]}{(N-1)\Delta t} \\ \ddot{\tau}_{kf(c)} &= \frac{\tau^l_{kf}[N] - \tau^l_{kf}[N-1] - \tau^l_{kf}[2] + \tau^l_{kf}[1]}{(N-2)\Delta t^2}\end{aligned} \tag{23}$$

Then the $E_{(c+i)}$ can be expressed as

$$E_{(c+i)} = \frac{\tau_{kf(c+i)} \cdot (1 - p_{(c+i)})}{R_{e(c)}} \tag{24}$$

$p_{(c+i)}$ represents the percentage of the knee torque target to be compensated by the assistive system. Therefore, the term $\tau_{kf(c+i)} \cdot (1 - p_{(c+i)})$ denotes the portion of the torque taken by the knee.

Since the system operates under low-dynamic motion conditions, we assume that the knee internal extensor mechanism remains approximately constant over the steps of the prediction horizon. Under this assumption, the relationship between muscle activation level $E_{(c+i)}$, which reflects muscle contraction force, and the knee internal torque $\hat{\tau}_{kf_{(c+i)}}$ can be approximated as linear.

To model this relationship, a constant ratio $R_{e(c)}$ is defined, which acts as a virtual moment arm converting knee internal torque $\hat{\tau}_{kf(c)}$ to muscle force, as indicated by the activation level $E_{(c)}$. The value of $R_{e(c)}$ is computed using:

$$R_{e(c)} = \frac{\hat{\tau}_{kf(c)}}{E_{(c)}} \tag{25}$$

The fatigue state $V_{(c+i)}$ in the predicate horizon can be formulated with the above formulations. Then the quadratic optimization problem can be formulated as

$$\begin{aligned}\min_u \; & J = K^T Q K + P^T R P \\ \text{s.t. } & 0 \le p_{(c+i)} \le p_{max} \\ & 5 \le F_{(c+i)} \le F_{max} \\ & -10 \le \Delta F_{(c+i)} \le 10\end{aligned} \tag{26}$$

where $K \in \mathbb{R}^{N\times 1}$ and $P \in \mathbb{R}^{N\times 1}$ are the state error and control input vectors, respectively. The matrices $Q \in \mathbb{R}^{N\times N}$ and $R \in \mathbb{R}^{N\times N}$ are diagonal, positive semi-definite weighting matrices used to penalize deviations in the cost function.

In this work, the elements $k_{(c+i)}$ of K is defined as

$$k_{(c+i)} = \frac{1}{V_m - V_{(c+i)}};\ (0 < V_m \le 1) \tag{27}$$

where the V_m is the preferred maximum muscle fatigue state. The resulting state error vector K in (26), is denoted as

$$K = \begin{bmatrix} k_{(c+1)} \\ k_{(c+2)} \\ \vdots \\ k_{(c+N)} \end{bmatrix} \in \mathbb{R}^{N\times 1} \tag{28}$$

During the operation, start from the beginning, the $V_{(c+i)}$ will increase from 0, indicating fully rest conditions. The $k_{(c+i)}$ will increase with the increase of $V_{(c+i)}$ and approaching to $+\infty$ when $V_{(c+i)}$ approaching to V_m. This will force the optimizer to raise the $p_{(c+i)}$ to mitigate the increase of $V_{(c+i)}$, until $p_{(c+i)}$ reaches the maximum allowed assistance level p_{max}. The choice of V_m should take into account the type of assistive device being used. For devices providing partial assistance, it is recommended to set $V_m = 1$, as the human muscle continues to contribute to joint torque in such scenarios, potentially leading to muscle fatigue decay. According to the definition in Equation (8), $V_{(c+i)}$ can asymptotically approach 1, but never exactly reach it. In contrast, for exoskeletons capable of providing full load support, it is appropriate to define $p_{\max} = 1$. In this case, the MFAC algorithm drives $p_{(c+i)}$ toward 1 as $V_{(c+i)}$ approaches V_m, indicating full assistance. This effectively allows the corresponding muscles to enter a recovery state. In such configuration, $V_{(c+i)}$ may closely approach V_m, but it will never exceed or equal it.

Accordingly, in this work, V_m is defined as 1, since the devices used provide partial assistance to the knee joint.

In (26), the Q, R are defined as

$$\begin{aligned}Q &= W \cdot w_r \\ R &= W \cdot (1 - w_r)\end{aligned} \tag{29}$$

where the W is a scaled identity matrix, while the w_r is a suppression factor predefined in the range $0-1$. A higher w_r will encourage the (26) to output with higher $p_{(c+i)}$ to mitigate the development of muscle fatigue. In contrast, the system will intend to have a lower assistance power input from the device, resulting in a lower electric power consumption.

In the defined optimization problem, three constraints were established: the feasible range of assistance level $p_{(c+i)}$, a tension force constraint that accounts for the Bowden tendon's minimum pretension and the maximum allowable force $F_{(c+i)}$ for safety, and a regulation on the rate of change of tension force $\Delta F_{(c+i)}$ to ensure smooth transitions. The tension force at each step is computed using

$$F_{(c+i)} = \frac{p_{(c+i)} \cdot \tau_{kf(c+i)}}{L_a\left(\theta_{kx(c)}\right)} \tag{30}$$

where $L_a(\theta_{kx(c)})$ represents the lever arm of the assistance device relative to the knee rotation center for the tension force. It is computed using the knee flexion angle $\theta_{kx(c)}$, measured just before the optimization begins. This value is assumed to remain constant throughout the optimization process for each step, given the slow motion speed and minimal variation in the lever arm within the prediction horizon. Furthermore, since $p_{(c+i)}$ and $F_{(c+i)}$ are linked via (30), the constraint on the rate of change of the tension force also ensures that $p_{(c+i)}$ does not change abruptly in optimization. Finally, the optimal force $F_{(c+1)}$ is provided to the low-level force controller as the reference force F_{ref} (illustrated in Fig. 6). Finally, the optimization problem is formulated using the C++ library CasADi [39] and solved with the nonlinear solver IPOPT. The optimization runs on a laptop equipped with an Intel Core i9-12900H CPU (up to 5.00 GHz). The average computation time per optimization step is 3.53 ms, which is well below the 10 ms required for the 100 Hz MFAC loop. The low-level force controller operates in a real-time thread at 1000 Hz under a Xenomai-patched Ubuntu system.

IEEE Transactions on Automation Science and Engineering (T-ASE) paper, presented at ICRA 2026, Vienna, Austria.

III. Experiments

Two main experiments were conducted to evaluate the proposed method. The first experiment aimed to demonstrate the training procedure of the muscle activation model. This experiment was performed with three male subjects, whose height and weight were as follows: [1.89 m, 90 kg] for subject $S1$, [1.74 m, 72 kg] for $S2$, and [1.76 m, 70 kg] for $S3$. The trained model from $S1$ was integrated into the knee joint assistance device (Exo-Muscle), alongside the muscle fatigue model and MFAC, to demonstrate the system's ability to estimate muscle activation and fatigue during human-robot interaction without EMG sensing, and to evaluate the performance of the muscle fatigue–aware controller.

Prior to each experimental trial, both in the human data collection experiments and the human experiments with the Exo-Muscle, the joint states obtained from IMU measurements were initialized to zero while the subject stood upright. For details on computing joint states using IMUs, please refer to Section II-A.

The entire experimental procedure was approved by the Liguria regional ethics committee: studio IIT-HRII-SOPHIA – N. CER Liguria 554/2020.

A. Human Data Collection

The first phase of the experiments involves acquiring human state data to train the muscle activation model. As detailed earlier, EMG signals from the Vastus Lateralis, along with knee flexion angle and torque, are collected. The EMG signal is captured using electrodes on the Vastus Lateralis, amplified with a Bagnoli EMG system (Delsys) at a gain of 1000, and sampled at 1000 Hz via an ADC board.

The sampled signal is processed with the following steps:

- Firstly, the signal is filtered via a Butterworth band-pass filter with cutoff frequencies of 20 Hz and 450 Hz.
- Then, the band-passed signal is rectified by taking its absolute value.
- A second-order low-pass filter with a cutoff frequency of 1 Hz is then applied to obtain the envelope of the rectified signal. The low-pass filter is applied both in forward and reverse directions to have a zero phase shift.
- Finally, the signal is normalized using (7).

To ensure the applicability of the trained model for most operating conditions in real working scenarios, the following four different motion patterns were selected to collect the human-related data.

- Motion 1 (M1): Stand to squat.
- Motion 2 (M2): Lift load (15 kg) from the ground to the desk at the lateral side of the subject.
- Motion 3 (M3): Lift load (15 kg) from the ground to the desk at the front of the subject.
- Motion 4 (M4): Step on stairs with different heights

Each motion pattern is repeated ten times. The normalized EMG signal (computed with (7)), knee flexion angle (measured with IMUs), and knee torque (computed with (3)) are used for the training of the model. Each subject performs the same motions for collecting their individual dataset. The datasets are resampled with the processes in the next section and then used to train the muscle activation estimation model.

TABLE I

RMSE of Measured and Estimated Muscle Activation Level for Each Subject and Each Designed Motion Pattern

		M1	M2	M3	M4	Total
S1	**Train**	0.029	0.050	0.061	0.071	0.055
	Test	0.051	0.081	0.065	0.073	0.066
S2	**Train**	0.055	0.048	0.046	0.096	0.065
	Test	0.063	0.056	0.066	0.142	0.089
S3	**Train**	0.046	0.037	0.040	0.048	0.043
	Test	0.042	0.049	0.043	0.051	0.046

B. Muscle Activation Estimation Model Training Experiment

To process the GPR, a suitable database is prepared. EMG data from the previous step is sampled at 1000 Hz, while joint state and knee torque are computed and sampled at 200 Hz. The EMG is then resampled at 200 Hz to match the knee joint angle and torque data. For model evaluation, the dataset is split equally, with the first half used for training and the second for validation. However, large datasets result in a large covariance kernel matrix, increasing computation time for estimating muscle activation M and introducing latency in the control system. Thus, the size of the training data set needs to be reduced to achieve a trade-off between computation and model accuracy. In this study, 250 data points are resampled for each motion pattern with equal space in the training data pool. In total, for the four motion patterns, 1000 training data points are collected. The training dataset for each motion from one subject is mixed and used to train a personalized GPR model. Then the trained GPR model is tested both with the training dataset and the testing dataset, which is resampled in the same way as the training dataset.

To evaluate the performance of the muscle activation model, the root means square error (RMSE) is defined in (31) and calculated for both the training and testing datasets.

$$RMSE = \sqrt{\frac{1}{N}\sum_{k=1}^{N} e_k^2} \tag{31}$$

The N is the number of data points for each motion pattern. The e_k is the difference between the measured value and the predicted value at the k^{th} data point. The RSME for each motion pattern and overall is computed for each subject and shown in Table I.

As shown in Table I, the RMSE for the testing dataset is generally higher than for the training dataset, since the trained model has already adapted to the training data. For each subject, the highest RMSE is observed during motion M4, which corresponds to stair climbing. Compared to the other tested motions, stair climbing exhibits greater complexity and variability, with EMG signals being sensitive to muscle contraction speed and occasional short artifacts caused by skin movement near the electrode. These factors increase signal variance and contribute to the higher RMSE observed in this motion.

IEEE Transactions on Automation Science and Engineering (T-ASE) paper, presented at ICRA 2026, Vienna, Austria.

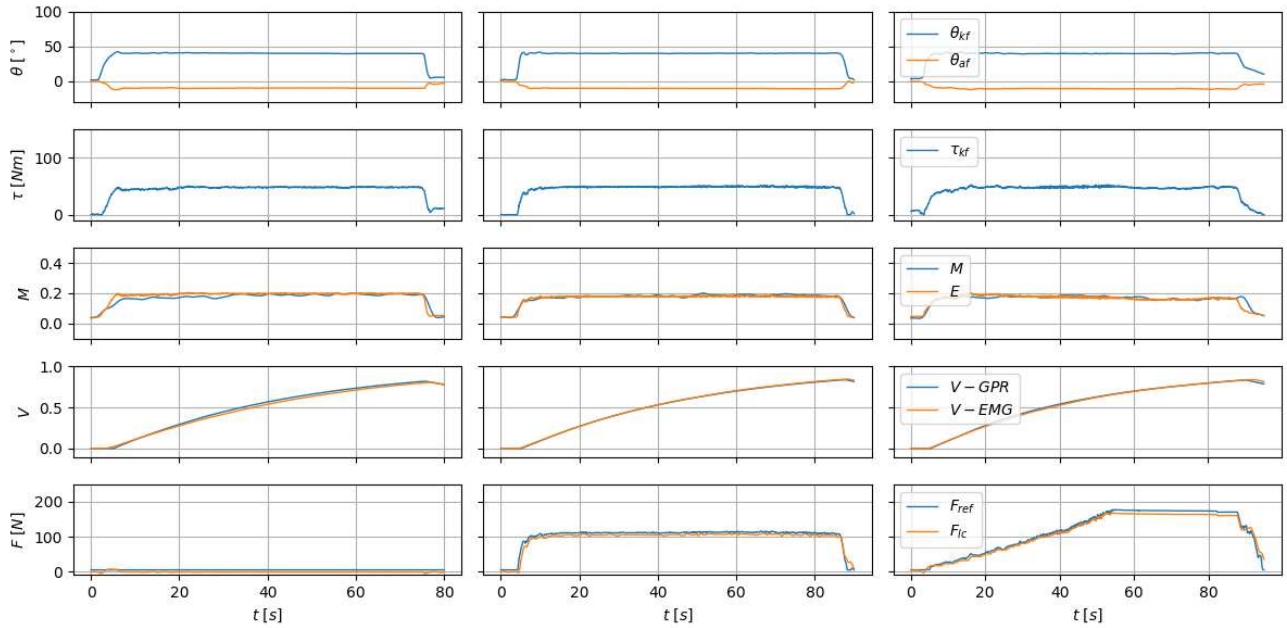

Fig. 7. Experimental results for the motion type static squat. (From left to right: first column indicates the experimental result without any assistance, the second column indicates the experimental result with a constant assistance level of 15%, the third column indicates the experimental result with MFAC.)

Nevertheless, the overall RMSE values for both the training and testing datasets remain relatively low, demonstrating good generalization performance of the trained model. This indicates that the model can reliably predict muscle activation using only the knee joint angle and torque as inputs. The following experiment, presented in the next section, further evaluates the trained model during operation of our Exo-Muscle knee assistive device, assessing its potential for use in real-time human–assistive device interaction scenarios.

C. Human Experiments With Exo-Muscle

This second experiment aims to evaluate the performance of the proposed MFAC controller and the online EMG-free muscle activation estimation model when the human subjects interact with the Exo-Muscle assistive device. In particular, in this experiment, the human subject wears the Exo-Muscle and performs three different types of motions (static squat, periodical squat, and stair stepping).

- The static squat experiments are conducted three times using the Exo-Muscle device: without assistance, with constant 15% knee torque compensation, and with the newly proposed MFAC. In each trial, the subject maintains a static squat position until the muscle fatigue index V reaches 0.8.
- In the periodical squat experiments, the subject performs a repeated stand-to-squat motion under two conditions: with constant 15% knee torque compensation and with the newly proposed MFAC. After reaching the squat position, the subject holds the pose for 3 seconds, then returns to a standing position and rests for 3 seconds before starting the next cycle. This sequence is repeated eight times.
- In the stair-stepping experiment, the subject repeatedly steps onto a brick using the leg fitted with the device, again under two conditions: with constant 15% knee torque compensation and with the newly proposed MFAC. After achieving the target pose, the subject holds it for 3 seconds, then returns to a standing position and rests for 2 seconds before the next cycle. This sequence is repeated eight times.

The experimental results of the static squat are shown in Fig. 7. The first column presents the results of the static squat experiment performed in the non-assistance mode, where the device applies only a $5\,N$ force to pre-tension the Bowden cable tendon. The second column shows the results under the constant knee torque compensation mode, in which a fixed percentage of knee torque τ_{kf} is compensated. The third column shows the results of the static squat using the proposed MFAC. In this mode, the maximum compensation level ($p_{\max}$) and maximum allowed tension force $F_{\max}$ were set to 0.3 and $180\,N$, respectively, as specified in (26). The constraints defined in the optimization account for both operational safety and the strength limits of the 3D-printed components in the Exo-Muscle drive train. The rows of Fig. 7, from top to bottom, display the ground reaction force, joint state, total knee joint moment, muscle activation (both estimated and measured), muscle fatigue index, and the reference and measured tension forces of the exoskeleton.

As shown in Fig. 7, knee flexion angle, ankle dorsiflexion angle (First row), and knee torque (second row) remain nearly identical across the static squat experiments under the different control modes. The fatigue index $v-GPR$ (fourth row) reaches the threshold of 0.8 after 66.95, 73.6, and 76.15 seconds in the non-assistance, 15% assistance, and MFAC control modes, respectively. This difference arises because, in the non-assistance mode, the tension force on the tendon (fifth row) is minimal, meaning the knee torque is entirely supported by

IEEE Transactions on Automation Science and Engineering (T-ASE) paper, presented at ICRA 2026, Vienna, Austria.

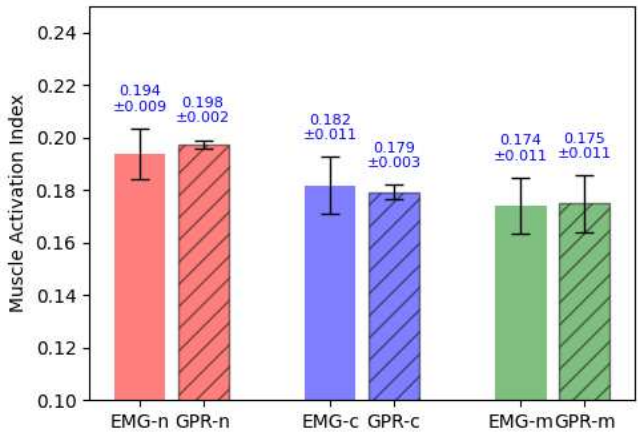

Fig. 8. The mean and standard deviation of muscle activation, measured by EMG and estimated by a GPR-trained model, when the subject is performing the static squat under non-assistance (n), constant assistance (c) and MFAC mode (m).

the subject's muscles. In contrast, under the assisted modes, the Exo-Mucle compensates for a portion of the knee torque, leading to lower muscle activation levels (third row) compared to the non-assistance condition. For the MFAC controller (the third column in Fig. 7), the initial tendon tension is much lower than in the constant assistance condition, in which phase the muscle fatigue builds faster. However, as the fatigue index V_t increases, the error in (27) grows rapidly. In response, the MFAC controller increases the assistance level to minimize the objective in (26), leading to a rise in the reference tension force, until it reaches the maximum tension force defined in the optimization, as the fatigue index increases (as shown in the sixth row of Fig. 7). To this end, we observe that both estimated and measured muscle activation gradually decrease as assistance increases, while at the same time, the muscle fatigue index rises more slowly than in the constant assistance case during the later phase of the squat. This results in a slightly longer time to reach the same level of muscle fatigue.

Although the time differences in reaching the maximum fatigue level are relatively small, the MFAC controller demonstrates a key advantage: it automatically adjusts the level of assistance based on the user's fatigue. In contrast, the fixed assistance mode requires careful and non-trivial tuning due to variations in task demands and individual user needs. The MFAC controller dynamically adapts to changing assistance requirements. Moreover, users can intuitively fine-tune the assistance response by adjusting the suppression factor in Eq. (29), enabling a more transparent, personalized, and effective operation.

Furthermore, in the static squat experiments, the average muscle activation levels obtained from both EMG measurements and trained model estimations were calculated during the stable squat phase. As shown in Fig. 8, the differences between the mean activation levels from EMG measurements and GPR model estimations are relatively small across all control modes. Both the measured (*EMG-C*) and estimated (*GPR-C*) muscle activation levels under constant assistance and MFAC are lower than those in the non-assistance mode, confirming that the assistance is effectively delivered to the knee joint. Because MFAC provides lower assistance during the initial stage of the squat and higher assistance during the later phase, the resulting average muscle activation level is slightly lower than that observed under constant assistance.

With respect to the standard deviation, the estimated values are generally much lower than the measured ones. The higher standard deviation observed in the estimations under the MFAC control mode is attributed to varying assistance levels, which result in changes in knee internal torque and, consequently, in the estimated muscle activation. These findings indicate that the trained model can accurately estimate muscle activation while simultaneously providing a more stable input (compared to EMG-measured muscle activation) for the muscle fatigue model.

The periodical squat and stair-stepping experiments are designed to assess the performance of the proposed controller, as well as the online EMG-free method for estimating muscle activation and fatigue during periodical tasks. In Fig. 9, the first two columns show the experimental results for the periodical squat with constant assistance and fatigue-based MPC, respectively, while the last two columns show the corresponding results for the stair-stepping motion. As seen in Fig. 9, the controller with constant assistance provides the same tension force profile across the phases of the motion. In contrast, the MFAC takes the fatigue state into account to provide adaptive assistance to the subject. As the fatigue index increases, the tension force observed in the later motion cycles becomes higher than that of the earlier cycles. As shown in the plot, the maximum tension force during the eighth motion cycle of both the periodical squat and stair-stepping is nearly three times greater than that of their first motion cycle. Due to the continuous adjustment of tension force is continuous, it keeps increasing even when the knee torque reaches its plateau phase in each motion cycle. The last row of Fig. 9 shows the system's power rate during operation. It can be observed that the system exhibits a similar power rate pattern across motion cycles in the test with constant assistance, whereas the power rate increases with the number of cycles in the test with MFAC.

The average power rate for each motion cycle is shown in Fig. 10. As seen in Fig. 10a for the periodical squat and Fig. 10b for the periodical stair-stepping, the power rate in the first motion cycle under constant assistance is more than four times higher than that under MFAC for the squat, and more than three times higher for the stair-stepping. As the number of motion cycles increases, the fatigue index also rises. Consequently, the power rate increases significantly, since the system is designed to provide more assistance when the fatigue index is higher. In contrast, under constant assistance, the average power rate for each motion cycle remains nearly the same across all eight motion cycles.

The periodical experiments successfully demonstrate that the proposed MFAC can effectively provide adaptive assistance to the user by accounting for muscle fatigue. Additionally, the fourth row of Fig. 7 and Fig. 9 shows that the measured

IEEE Transactions on Automation Science and Engineering (T-ASE) paper, presented at ICRA 2026, Vienna, Austria.

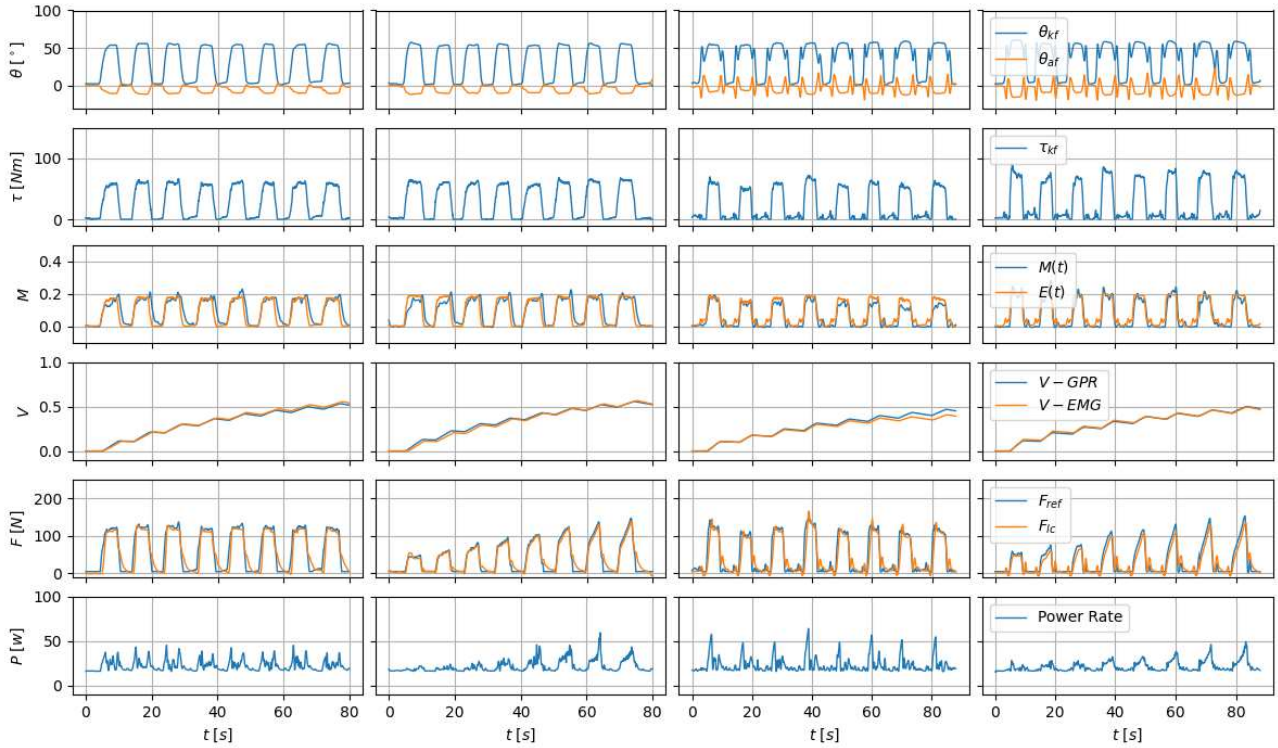

Fig. 9. Experimental results for the periodical motions. (The first and second columns show the experimental results for periodical squats with a constant assistance level of 15% and with MFAC, respectively, while the third and fourth columns show the experimental results for stair stepping with a constant assistance level of 15% and with MFAC, respectively.)

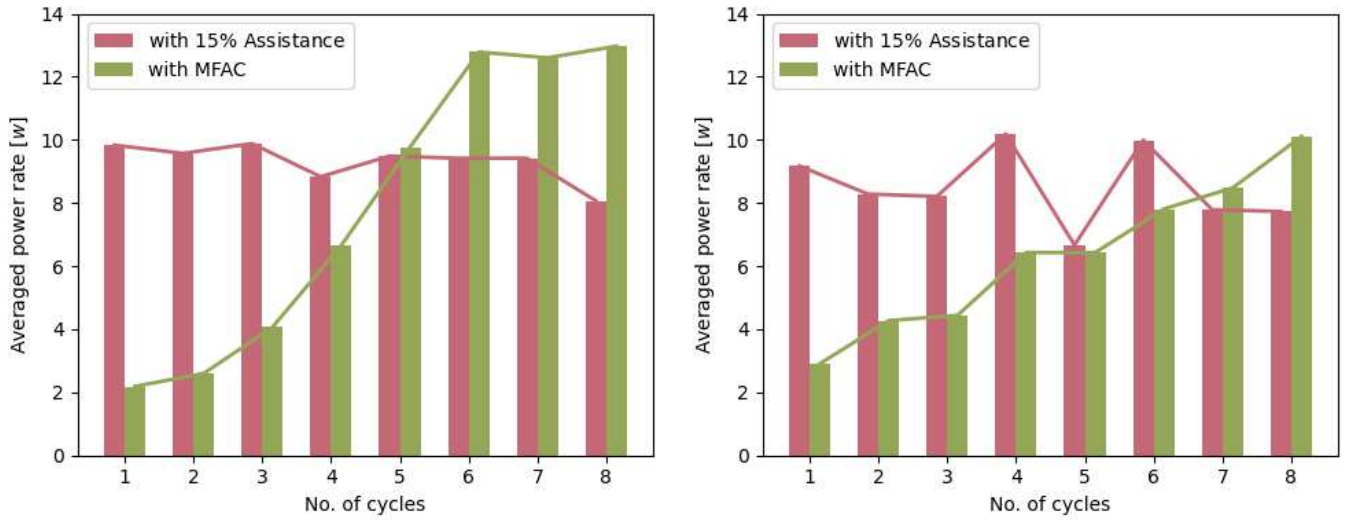

Fig. 10. (a) Averaged power rate for each motion cycle of periodical squat. (b) The average power rate for each motion cycle of periodical stair stepping.

and predicted muscle activation levels closely overlap, indicating that the trained model can reliably estimate muscle activation. Furthermore, in the fifth row of Fig. 9, across all four periodical motion trials, the evaluated muscle fatigue effectively transitions between fatigue accumulation mode, where $V-GPR$ increases, and recovery mode, where $V-GPR$ gradually decreases, depending on the state of the human knee joint.

Moreover, in both the static squat (Fig. 7) and periodic motion experiments (Fig. 9), the EMG-measured muscle activation levels were used as inputs to the same muscle fatigue model to obtain $V-EMG$. The resulting $V-EMG$ curves exhibit the same overall trend and almost completely overlap with $V-GPR$, indicating that the fatigue model driven by estimated muscle activation yields results nearly identical to those obtained using measured muscle activation.

IEEE Transactions on Automation Science and Engineering (T-ASE) paper, presented at ICRA 2026, Vienna, Austria.

These results demonstrate that the proposed approach and trained model can consistently estimate muscle activation without requiring a complex human joint model. Furthermore, they effectively demonstrate that the predicted muscle activation index can serve as input to the muscle fatigue model. Since the muscle activation estimation requires EMG measurements only during the offline training, the proposed approach enables the implementation of a human joint model-free and EMG-free tool for online muscle fatigue evaluation. This is particularly advantageous for real-world applications as it eliminates the need for EMG-based interfaces and their associated ergonomic constraints and uncertainties.

IV. Conclusion and Future Work

In this work, we presented a fatigue-aware adaptive controller. To support stable and reliable muscle fatigue evaluation, we first develop an online EMG-free muscle activation estimation method for muscle fatigue evaluation. The proposed approach employs GPR to train a muscle activation estimation model offline using EMG-recorded muscle activation, joint moment, and joint configuration data obtained from sensor measurements and kinematic computations. Once trained, the model can estimate muscle activation online using only human joint state and moment, data, eliminating the need for fragile and ergonomically intrusive EMG measurements during the deployment.

In validation experiments, the model was trained on data collected from various motion scenarios performed by human subjects. The experimental results demonstrate that the trained model can estimate muscle activation with high accuracy, as shown in Table I and the EMG plots in Fig. 7 and Fig. 9. The trained model is subsequently integrated into the control loop of a semi-rigid knee exoskeleton, serving as input for both the muscle fatigue estimation and the proposed MFAC.

Additional experimental results demonstrate that the trained model consistently estimates muscle activation, effectively supporting the muscle fatigue model in assessing the fatigue state of the engaged muscles. The MFAC subsequently provides smooth adaptive assistance tailored to the fatigue level of the user, helping mitigate the development of muscle fatigue. Notably, the MFAC enables the assistance device to reduce assistance and energy consumption when the user is in a low-fatigue state, where the risk of work-related musculoskeletal disorders is minimal, and to provide increased assistance with higher energy expenditure when the user is in a high-fatigue state, where the risk of such disorders is higher. This indicates that by accounting for the user's muscle fatigue state, the MFAC helps optimize energy use, potentially extending the device's operational time on a single battery charge.

Compared with prior works on muscle fatigue estimation, our approach builds upon Peternel's online fatigue assessment model [17], which directly relies on online muscle activation measurements via EMG, establishing a transparent link, since fatigue is inherently induced by muscle activation. In different, our method estimates muscle activation online using an offline-trained GPR model, which captures the relationship between joint state and muscle activity. As shown in Table I and Fig. 8, the trained model provides estimates of muscle activation that are sufficiently accurate and more stable than those obtained from direct online EMG measurements. This robustness makes our approach more suitable for industrial assistance scenarios than either EMG-based methods [17] or ultrasound-based approaches [29]. Furthermore, different from the methods in [28], and [30], our GPR-based muscle activation estimation model is subject-specific, enabling personalized adaptation without the need for detailed joint-level biomechanical models.

From a control standpoint, we integrate the estimated effect of muscle fatigue into an optimization-based adaptive control framework. Different from prior works [17], [28], [29], [30], our optimization-based approach for managing assistance not only accounts for the current fatigue state but also proactively optimizes continuous assistance by considering the progression trend of fatigue and incorporating key system constraints, such as force limits and bounds on the rate of assistance change. This design ensures smooth and safe adaptation, as validated through both static and periodic motion experiments. Moreover, as indicated by (26) and (29), the framework has the potential to support online user tuning of the optimizer's response via the suppression factor w_r, with the designed constraints ensuring smooth transitions before and after tuning. This capability follows directly from the optimization problem formulation, although it has not yet been experimentally validated.

Furthermore, to the best of our knowledge, the energy-related benefits of fatigue-aware adaptive control have not been investigated in prior work. In our experiments, we demonstrate that the semi-rigid assistive device controlled with MFAC conserves energy by reducing support when the user is less fatigued and increasing support as fatigue develops. Consequently, MFAC not only mitigates fatigue progression but also inherently regulates power and energy output according to the user's actual demand, thereby potentially extending the operational time of mobile assistive devices under a fixed battery capacity.

However, currently, the muscle activation model is trained using standard GPR, whose computational cost increases significantly with the number of training data points, especially in more complex scenarios. To address this limitation, future work will explore more advanced GP methods, such as inducing point techniques, variational inference approaches, and structured kernel interpolation. These methods can substantially reduce the computational burden while preserving much of GPR's expressive power. Moreover, the proposed method requires a one-time EMG-based calibration before deployment, which is feasible in industrial settings using portable EMG systems. To reduce reliance on subject-specific calibration and broaden applicability, we plan to investigate generalized cross-subject models trained on data from multiple individuals. In addition, we aim to extend the proposed approach to multi-degree-of-freedom (multi-DoF) exoskeletons and evaluate its performance with multiple subjects in real-world applications, such as logistics palletizing tasks in industrial environments.

IEEE Transactions on Automation Science and Engineering (T-ASE) paper, presented at ICRA 2026, Vienna, Austria.

REFERENCES

[1] S. Braganca, E. Costa, I. Castellucci, and P. M. Arezes, *A Brief Overview of the Use of Collaborative Robots in Industry 4.0: Human Role and Safety*. Cham, Switzerland: Springer,2019.

[2] J. Frohm, V. Lindström, J. Stahre, and M. Winroth, "Levels of automation in manufacturing," *Ergonomia-Int. J. Ergonom. Hum. Factors*, vol. 30, no. 3, pp. 181–207, Jan. 2008.

[3] L. Punnett and D. H. Wegman, "Work-related musculoskeletal disorders: The epidemiologic evidence and the debate," *J. Electromyogr. Kinesiol.*, vol. 14, no. 1, pp. 13–23, Feb. 2004.

[4] B. P. Bernard and V. Putz-Anderson, *Musculoskeletal Disorders and Workplace Factors: A Critical Review of Epidemiologic Evidence for Work-Related Musculoskeletal Disorders of the Neck, Upper Extremity, and Low Back* (NIOSH Numbered Publications). National Institute for Occupational Safety and Health, Jul. 1997. [Online]. Available: https://stacks.cdc.gov/view/cdc/21745

[5] T. J. Armstrong et al., "A conceptual model for work-related neck and upper-limb musculoskeletal disorders," *Scandin. J. work*, vol. 19, no. 2, pp. 73–84, 1993.

[6] S. Mclean and J. Samorezov, "Fatigue-induced acl injury risk stems from a degradation in central control," *Medicine Sci. Sports Exerc.*, vol. 41, no. 8, p. 1662, 2009.

[7] J. de Kok et al., "Work-related musculoskeletal disorders: Prevalence, costs and demographics in the EU," in *European Statistics on Accidents at Work*. European Health, 2013, doi: 10.2802/66947. [Online]. Available: http://europa.eu

[8] G. Sjøgaard, "Intramuscular changes during long-term contraction," in *The Ergonomics of Working Postures*. London, U.K.: Taylor & Francis, 1986, pp. 136–143. [Online]. Available: https://www.taylorfrancis.com/chapters/edit/10.1201/b12565-14/intramuscular-changes-long%E2%80%93term-contraction-gisela-sj%C3%B8gaard

[9] H.-J. Shin and J.-Y. Kim, "Measurement of trunk muscle fatigue during dynamic lifting and lowering as recovery time changes," *Int. J. Ind. Ergonom.*, vol. 37, no. 6, pp. 545–551,Jun. 2007.

[10] S. De Bock et al., "An occupational shoulder exoskeleton reduces muscle activity and fatigue during overhead work," *IEEE Trans. Biomed. Eng.*, vol. 69, no. 10, pp. 3008–3020, Oct. 2022.

[11] E. P. Lamers, J. C. Soltys, K. L. Scherpereel, A. J. Yang, and K. E. Zelik, "Low-profile elastic exosuit reduces back muscle fatigue," *Sci. Rep.*, vol. 10, no. 1, p. 15958, Sep. 2020.

[12] N. V. Divekar, G. C. Thomas, A. R. Yerva, H. B. Frame, and R. D. Gregg, "A versatile knee exoskeleton mitigates quadriceps fatigue in lifting, lowering, and carrying tasks," *Sci. Robot.*, vol. 9, no. 94, p. 8282, Sep. 2024.

[13] R. H. Fitts, "The cross-bridge cycle and skeletal muscle fatigue," *J. Appl. Physiol.*, vol. 104, no. 2, pp. 551–558, Feb. 2008.

[14] J. Z. Liu, R. W. Brown, and G. H. Yue, "A dynamical model of muscle activation, fatigue, and recovery," *Biophysical J.*, vol. 82, no. 5, pp. 2344–2359, May 2002.

[15] Y. Giat, J. Mizrahi, and M. Levy, "A musculotendon model of the fatigue profiles of paralyzed quadriceps muscle under FES," *IEEE Trans. Biomed. Eng.*, vol. 40, no. 7, pp. 664–674,Jul. 1993.

[16] C. J. D. Luca, "Myoelectrical manifestations of localized muscular fatigue in humans," *Crit. Rev. Biomed. Eng.*, vol. 11, no. 4, pp. 251–79, 1984.

[17] L. Peternel, N. Tsagarakis, D. Caldwell, and A. Ajoudani, "Robot adaptation to human physical fatigue in human–robot co-manipulation," *Auto. Robots*, vol. 42, no. 5, pp. 1011–1021,Jun. 2018.

[18] L. Ma, D. Chablat, F. Bennis, W. Zhang, and F. Guillaume, "A new muscle fatigue and recovery model and its ergonomics application in human simulation," *Virtual Phys. Prototyping*, vol. 5, no. 3, pp. 123–137,Sep. 2010.

[19] B. J. Carnahan, B. A. Norman, and M. S. Redfern, "Incorporating physical demand criteria into assembly line balancing," *IIE Trans.*, vol. 33, no. 10, pp. 875–887, Oct. 2001.

[20] D. D. Wood, D. L. Fisher, and R. O. Andres, "Minimizing fatigue during repetitive jobs: Optimal work-rest schedules," *Human Factors, J. Human Factors Ergonom. Soc.*, vol. 39, no. 1, pp. 83–101,Mar. 1997.

[21] D. M. Thompson, "Kinesiology of the musculoskeletal system: Foundations for physical rehabilitation," *Phys. Therapy*, vol. 83, no. 4, p. 402,2003.

[22] W. Herzog and L. Read, "Lines of action and moment arms of the major force-carrying structures crossing the human knee joint," *J. Anatomy*, vol. 182, no. 2, pp. 213–230, 1993.

[23] H. Iwaki, V. Pinskerova, and M. A. R. Freeman, "Tibiofemoral movement 1: The shapes and relative movements of the femur and tibia in the unloaded cadaver knee," *J. Bone Joint Surg. Brit. volume*, vol. 82, no. 8, pp. 1189–1195, Nov. 2000.

[24] L. Ma, D. Chablat, F. Bennis, and W. Zhang, "A new simple dynamic muscle fatigue model and its validation," *Int. J. Ind. Ergonom.*, vol. 39, no. 1, pp. 211–220, Jan. 2009.

[25] M. Qu et al., "Continuously monitoring of muscle fatigue based on a wearable micromachined ultrasonic transducer probe," *Sens. Actuators A, Phys.*, vol. 365, Jan. 2024, Art. no.114892.

[26] H. Turker and H. Sözen, "Surface electromyography in sports and exercise," in *Electrodiagnosis in New Frontiers of Clinical Research*, H. Turker, Ed., London, U.K.: IntechOpen, 2013, ch. 9, doi: 10.5772/56167.

[27] L. Peternel, C. Fang, N. Tsagarakis, and A. Ajoudani, "A selective muscle fatigue management approach to ergonomic human–robot co-manipulation," *Robot. Comput.-Integr. Manuf.*, vol. 58, pp. 69–79, Aug. 2019.

[28] A. J. Del-Ama, Á. Gil-Agudo, J. L. Pons, and J. C. Moreno, "Hybrid FES-robot cooperative control of ambulatory gait rehabilitation exoskeleton," *J. NeuroEng. Rehabil.*, vol. 11, no. 1, p. 27,2014.

[29] Z. Sheng, A. Iyer, Z. Sun, K. Kim, and N. Sharma, "A hybrid knee exoskeleton using real-time ultrasound-based muscle fatigue assessment," *IEEE/ASME Trans. Mechatronics*, vol. 27, no. 4, pp. 1854–1862, Aug. 2022.

[30] L. Bergmann, L. Hansmann, P. von Platen, S. Leonhardt, and C. Ngo, "Fatigue assessment and control with lower limb exoskeletons," *IEEE Trans. Hum.-Mach. Syst.*, vol. 55, no. 1, pp. 10–22,Feb. 2025.

[31] Y. Zhang, A. Ajoudani, and N. G. Tsagarakis, "Exo-muscle: A semi-rigid assistive device for the knee," *IEEE Robot. Autom. Lett.*, vol. 6, no. 4, pp. 8514–8521, Oct. 2021.

[32] L. Saccares, I. Sarakoglou, and N. G. Tsagarakis, "A novel joint torque estimation method and sensory system for assistive lower limb exoskeletons," in *Proc. IEEE/RSJ Int. Conf. Intell. Robots Syst. (IROS)*, Oct. 2018, pp. 1–9.

[33] P. de Leva, "Adjustments to Zatsiorsky–Seluyanov's segment inertia parameters," *J. Biomechanics*, vol. 29, no. 9, pp. 1223–1230,Sep. 1996.

[34] V. Zatsiorsky and V. Seluyanov, "The mass and inertia characteristics of the main segment of human body," in *Proc. 8th Int. Congr. Biomechanics, Human Kinetics Publishers Champaign*, Oct. 1983, vol. 56, no. 2, pp. 1152–1159.

[35] J. Ding, A. S. Wexler, and S. A. Binder-Macleod, "A predictive model of fatigue in human skeletal muscles," *J. Appl. Physiol.*, vol. 89, no. 4, pp. 1322–1332, Oct. 2000.

[36] N. Hogan, "Adaptive control of mechanical impedance by coactivation of antagonist muscles," *IEEE Trans. Autom. Control*, vol. AC-29, no. 8, pp. 681–690, Aug. 1984.

[37] B. A. Alkner, P. A. TescH, and H. E. Berg, "Quadriceps EMG/force relationship in knee extension and leg press," *Med. Sci. Sports Exerc.*, vol. 32, no. 2, pp. 459–463, Feb. 2000.

[38] D. M. Pincivero, V. Gandhi, M. K. Timmons, and A. J. Coelho, "Quadriceps femoris electromyogram during concentric, isometric and eccentric phases of fatiguing dynamic knee extensions," *J. Biomechanics*, vol. 39, no. 2, pp. 246–254, 2006.

[39] J. A. E. Andersson, J. Gillis, G. Horn, J. B. Rawlings, and M. Diehl, "CasADi: A software framework for nonlinear optimization and optimal control," *Math. Program. Comput.*, vol. 11, no. 1, pp. 1–36,Mar. 2019.

Yifang Zhang (Member, IEEE) received the M.Sc. degree in mechanical engineering from The University of Sheffield, Sheffield, U.K., in 2016, and the Ph.D. degree from the Humanoid and Human-Centered Mechatronics (HHCM) Research Line, Istituto Italiano di Tecnologia (IIT), Genoa, Italy, in 2023. Since 2023, he has been a Post-Doctoral Researcher at HHCM Research Line, IIT. His current research interests include the design, modeling, and control of physical assistive devices and legged robots.

IEEE Transactions on Automation Science and Engineering (T-ASE) paper, presented at ICRA 2026, Vienna, Austria.

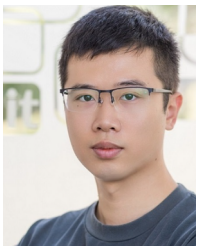

Jingcheng Jiang received the M.Sc. degree in control engineering from the University of Chinese Academy of Sciences, Beijing, China, in 2021. He is currently pursuing the Ph.D. degree with the Humanoid and Human-Centered Mechatronics Research Line, Istituto Italiano di Tecnologia (IIT), University of Genoa, Genoa, Italy.

His current research interests include the mechatronics design and control of legged robots and wearable devices.

Arash Ajoudani (Member, IEEE) is currently the Director of the Human-Robot Interfaces and Interaction Laboratory, IIT. He is the author of the book *Transferring Human Impedance Regulation Skills to Robots* (Springer Tracts in Advanced Robotics—STAR) and several publications in journals, international conferences, and book chapters. From 2022 to 2024, he was an Elected IEEE RAS AdCom Member and the Chair and Representative of the IEEE-RAS Young Professionals Committee. He was a recipient of European Research Council (ERC) starting grant 2019 (Ergo-Lean), the Coordinator of the Horizon-2020 Project SOPHIA, the Co-Coordinator of the Horizon-2020 Project CONCERT, and the Principal Investigator of the HORIZON-MSCA Project RAICAM. He was a recipient of the IEEE Robotics and Automation Society (RAS) Early Career Award in 2021. He is a Senior Editor of *The International Journal of Robotics Research*.

Nikos G. Tsagarakis is currently a tenured Senior Scientist and the Principal Investigator of the Humanoid and Human Centred Mechatronics (HHCM) Research Line, a leading research laboratory at IIT, with a strong expertise in robot design, modeling, and control, and in the development of new mechatronics components (actuation and sensing). He was the Coordinator of the EU Project WALKMAN. He is currently the Coordinator of the EU Project CONCERT. He has also served as the principal investigator for several EU projects in the past. He is the author or co-author of over 400 papers in research journals and at international conferences and holds 16 patents. He has been in the Program Committee of several international conferences, including IEEE ICRA, IROS, RSS, HUMANOIDS BIOROB, and ICAR. He was the Technical Editor of IEEE/ASME TRANSACTIONS ON MECHATRONICS from 2012 to 2015. He has served on the editorial board for IEEE ROBOTICS AND AUTOMATION LETTERS from 2014 to 2019. He is currently a Senior Editor of IEEE/ASME TRANSACTIONS ON MECHATRONICS.

Open Access funding provided by 'Istituto Italiano di Tecnologia' within the CRUI CARE Agreement